J Pharmacol Sci **120**, 228 – 240 (2012)

Journal of Pharmacological Sciences

Full Paper

Evaluation of the Protective Effects of Cyclosporin A and FK506 on Abnormal Cytosolic and Mitochondrial Ca^{2+} Dynamics During Ischemia and Exposure to High Glutamate Concentration in Mouse Brain Slice Preparations

Tomoharu Yokoyama[1], Tadashi Tanoue[2], Erika Hasegawa[3], Yukio Ikeda[1], Shouichi Ohta[1], Akibumi Omi[4], Yoshihisa Kudo[3,*], and Hiroyuki Uchino[4]

[1]*Department of Emergency and Critical Care Medicine and Neurosurgery, Tokyo Medical University Hachioji Medical Center, 1163 Tatemachi, Hachioji, Tokyo 193-0998, Japan*
[2]*Department of Anesthesiology, Kumamoto Regional Medical Center, 5-16-10 Honjo, Kumamoto 860-0811, Japan*
[3]*School of Life Science, Tokyo University of Pharmacy and Life Sciences, 1432-1 Horinouchi, Hachioji, Tokyo 192-0032, Japan*
[4]*Department of Anesthesiology, Tokyo Medical University, 6-7-1 Nishishinjuku, Shinjuku-ku, Tokyo 160-0023, Japan*

Received June 24, 2012; Accepted September 24, 2012

Abstract. We examined the protective effects of the immunosuppressants cyclosporin A (CsA) and FK506 on abnormal cytosolic Ca^{2+} ($[Ca^{2+}]c$) and mitochondrial Ca^{2+} concentration ($[Ca^{2+}]m$) dynamics induced by ischemia or high L-glutamate concentration in mouse brain slice preparations. We used fura-4F and rhod-2 as indicators for $[Ca^{2+}]c$ and $[Ca^{2+}]m$, respectively, in their acetoxymethylester form. Slice preparations loaded with either of these two indicators were exposed to ischemic artificial cerebrospinal fluid (oxygen- and glucose-deprived medium) for 12 min or to aerobic medium with high L-glutamate concentration (isotonic 20 mM L-glutamate) for 5 min. CsA (1 – 10 μM) showed significant protective effects on the maximum increase in ischemia-induced $[Ca^{2+}]c$ and $[Ca^{2+}]m$. FK506 (10 μM) showed significant protective effects on the $[Ca^{2+}]m$ increase, but not on the ischemia-induced $[Ca^{2+}]c$ increase. Both immunosuppressants showed almost equal protective effects on the $[Ca^{2+}]c$ and $[Ca^{2+}]m$ increases induced by high L-glutamate concentration. These results suggest that the protective effects of CsA and FK506 on Ca^{2+} overloading may be dependent upon the common pharmacological sites of actions relating to their effects as immunosuppressants. The small, but significant depressant effects of these drugs could give us important clues for rescuing critical brain damage induced by Ca^{2+} overloading.

Keywords: ischemia, glutamate, Ca^{2+} overloading, cyclosporin A, FK506

Introduction

Since intracellular Ca^{2+} is widely used as a second messenger (1), the ion must be rapidly extruded after performing its function to maintain a suitable intracellular environment for subsequent signal transduction (2, 3). Mitochondria, vitally important organelles that function as centers of energy metabolism, use a Ca^{2+} uniporter located on the inner membrane to sequester accumulated cytosolic Ca^{2+} ($[Ca^{2+}]c$) (4). Mitochondria also work as decoders of Ca^{2+} signals for energy production (5 – 7).

In highly energy-dependent cells (e.g., neuronal cells), the deficiency of an energy source disrupts the ion homeostasis of intracellular environments, which subsequently induces membrane depolarization and facilitates Ca^{2+} influx from the extracellular space through opened voltage-sensitive Ca^{2+} channels (8 – 9). Ca^{2+} influx into neuronal cells is induced by the activation of glutamate receptors, which are stimulated by a large amount of glutamate released from neuronal cells themselves following depolarization (10, 11).

The massive increase in Ca^{2+} concentration due to an

*Corresponding author. kudoy@toyaku.ac.jp
Published online in J-STAGE on October 26, 2012 (in advance)
doi: 10.1254/jphs.12145FP

energy deficit in cells eventually saturates the Ca^{2+} capacity of mitochondria within a few minutes. The saturated mitochondria open channels referred to as mitochondrial permeability transition pores (mPTPs), which are permeable to molecules less than 1500 Da (12 – 16). Once these mPTPs are opened, mitochondria will lose their capacity for Ca^{2+} sequestration, resulting in an abnormal increase in intracellular Ca^{2+} concentration ($[Ca^{2+}]i$). The increased $[Ca^{2+}]i$ subsequently triggers Ca^{2+}-dependent enzymes associated with superoxide production (17, 18) and the breakdown of phospholipids and proteins (19, 20). Following Ca^{2+}-dependent enzyme activation, these enzymes induce severe breakdown of functional molecules, the cytoskeleton, and the plasma membrane, causing acute neuronal cell death (necrosis). Even if the cells exposed to a sharp increase in $[Ca^{2+}]i$ were to be rescued by a resupply of energy, most of these cells would die in subsequent slow processes (i.e., apoptosis) (21, 22).

Clinically, we encounter various types of energy-deficit induced brain damage, such as damage caused by disruption and thrombosis in brain blood vessels, asphyxia, carbon monoxide poisoning, or severe hypoglycemia. However, drugs that can be used to rescue patients from such a state are limited.

Cyclosporin A (CsA) and FK506, well known immunosuppressants, have been reported to have protective effects on experimental brain damage induced by ischemia (23 – 26). Although there are conflicting reports regarding their efficacy, these immunosuppressants have long been expected to yield important clues for developing new drugs that could rescue the brain from ischemic damage. CsA and FK506 inhibit the activity of calcineurin, an abundant phosphatase (27). However, the advantageous effects of these drugs on neuronal damage cannot be ascribed simply to their inhibitory effects on the enzyme. Since CsA interacts with cyclophilin D, an immunophilin and a component molecule of mPTPs (28, 29), the main site of CsA action is the mitochondrion (30). On the other hand, FK506 interacts with an FK506-binding protein, a member of the immunophilin protein family distinct from mPTPs (31, 32).

In the present study, we investigated the underlying mechanisms of the different effects of CsA and FK506 on brain damage. Specifically, we examined the $[Ca^{2+}]c$ and mitochondrial Ca^{2+} concentrations ($[Ca^{2+}]m$) in mouse brain slice preparations by loading them with fura-4F and rhod-2, respectively, in their acetoxymethylester form.

We used "macro" imaging on a device consisting of a conventional fluorescence microscope with a low magnification objective lens and an image processor (33). By this method, we could evaluate Ca^{2+} dynamics in wide areas of the slice preparations when exposed to an ischemic condition or high L-glutamate concentration in a single experiment. The specific vulnerability of the hippocampal CA1 (CA1) region to ischemia and its Ca^{2+} dependency has been reported as early as 1982 (34), but the reasons for this phenomenon still remain poorly understood. We attempted to compare the $[Ca^{2+}]c$ and $[Ca^{2+}]m$ dynamics and the effects of drugs in the cerebral cortex and CA1 region under abnormal conditions. We expected to find some clues to explain the regional differences in vulnerability and drug effects.

Materials and Methods

Fresh mouse brain slice preparation

The study protocol was approved by the Institutional Animal Care Committee of Tokyo Medical University, which follows the "Guidance Principles for the Care and Use of Laboratory Animals" approved by The Japanese Pharmacological Society. Male adult C57BL/6N mice (1 – 3-month-old) were kept in an animal room where light was artificially controlled from 7:00 AM to 7:00 PM and temperature was maintained at 26°C ± 1°C. The animals were allowed to take food and water ad libitum.

Mice were decapitated under ether anesthesia. The whole brain was immediately isolated and kept in ice-cold aerobic artificial cerebrospinal fluid (ACSF) for 10 min. Then, 300-μm horizontal brain slices, including the ventral hippocampus and lateral cerebral cortex (LC), were prepared using a tissue slicer (DTK-1000; Dosaka EM Co., Ltd., Kyoto). The slices were separated into right and left pieces and used as hemi-brain preparations randomly.

Staining of slice preparations with Ca^{2+} indicators

Three or four pieces of slice preparations were placed into ACSF containing either of the fluorescence Ca^{2+} indicators (5 μM fura-4F/AM or 3 μM rhod-2/AM) at room temperature (25°C ± 2°C for 45 min. The preparations were then transferred to fresh ACSF and incubated for at least 30 min before use. During and after staining, the ACSF was aerated constantly with 95% O_2 and 5% CO_2 at room temperature.

Ca^{2+} measurement by imaging analysis

Slice preparations stained with either of the Ca^{2+} indicators were placed in a recording chamber that was fixed on the stage of an inverted microscope (IX71; Olympus Co., Tokyo), and they were constantly perfused (2 mL/min) with fresh ACSF aerated with 95% O_2 and 5% CO_2 using a micro tube pump (MP-32; Tokyo Rikakikai Co., Ltd., Tokyo).

The fluorescence images of the slice preparations were detected using a CCD camera (Orca-ER; Hamamatsu Photonics K.K., Hamamatsu, Shizuoka) through the 4 × objective lens of the inverted microscope. Two-dimensional images of a hemi-brain slice preparation were processed by an image processing system using specific software (Aquacosmos; Hamamatsu Photonics).

The time courses of the changes in $[Ca^{2+}]i$ at two regions of interest (ROI), specifically the LC and CA1 regions, were calculated as the average brightness contained within an area of 50 × 50 pixels (about 1 mm^2 of the slice preparation) of each ROI. For the preparation loaded with fura-4F, the ratio of the fluorescence (> 500 nm) induced by alternative excitation at 340 nm versus 380 nm (F340/F380) was calculated. In the rhod-2–stained preparations, the ratio of the fluorescence (> 580 nm) induced by an excitation wavelength of 540 nm was calculated by taking the initial image as a reference.

Composition of experimental medium

Normal aerobic ACSF had the following composition: 124.0 mM NaCl, 26.0 mM $NaHCO_3$, 2.5 mM KCl, 2.0 mM $CaCl_2$, 1.0 mM $MgCl_2$, 1.25 mM NaH_2PO_4, and 10.0 mM D-glucose; the solution was aerated with 95% O_2 and 5% CO_2. The ischemic ACSF had the following composition: 124.0 mM NaCl, 26.0 mM $NaHCO_3$, 2.5 mM KCl, 2.0 mM $CaCl_2$, 1.0 mM $MgCl_2$, 1.25 mM NaH_2PO_4, and 10.0 mM 2-deoxy-D-glucose; the solution was aerated with 95% N_2 and 5% CO_2.

L-Glutamate (5 – 30 mM) containing ACSF was prepared by diluting isotonic 100 mM L-glutamate–ACSF, which was prepared by substituting 100 mM NaCl with 100 mM L-glutamate monosodium salt.

Isotonic 80 mM (80K) potassium ACSF was prepared by substituting 77.5 mM NaCl in normal ACSF with 77.5 mM KCl.

Ischemia (hypoxia and hypoglycemia) was induced by replacing the normal medium with ischemic ACSF for 12 min. The temperature of the medium was maintained at 30°C ± 1°C using a self-made temperature control unit that had been previously tested for reliability.

Evaluation of Ca^{2+} dynamics in control and drug-treated slice preparations during and after exposure to ischemia and L-glutamate

In the present study, F340/F380 data for fura-4F and F540/F540 data for rhod-2 were mathematically normalized to 1.0 at the data point just before exposure to ischemia. We examined the Ca^{2+} concentrations in the LC and CA1 regions before, during, and after exposure to ischemia, and the data obtained in separate slice preparations were averaged with time. We expressed the maximum increase in Ca^{2+} concentration, detected as F340/F380 (fura-4F) or F540/F540 (rhod-2), during ischemia as the ratio of increased to resting concentration. We evaluated the effects of CsA and FK506 by applying them to the mouse brain slice preparations 10 min before the induction of ischemia up to the end of the experiments. We added 0.1% DMSO to both ACSF media as a vehicle control for CsA and FK506.

Evaluation of drug effects on slice preparations exposed to high glutamate concentrations using Ca^{2+} indicators

We examined the dynamic fluorescence changes during exposure to extremely high concentrations of L-glutamate. In this experiment, we exposed the preparation to 5 – 30 mM L-glutamate ASCF for 5 min. We examined the protective effects of CsA and FK506 on the L-glutamate–induced fluorescence dynamics in the slice preparations loaded with fura-4F or rhod-2. We also investigated the fluorescence dynamics on the slice preparations loaded with MitoTracker Red (3 μM).

Drugs

CsA (MW 1202.61) and FK506 monohydrate (MW 822.03) were purchased from Sigma (St. Louis, MO, USA). MitoTracker Red was procured from Lonza Walkersville, Inc. (Walkersville, MD, USA). These drugs were dissolved in DMSO (Sigma-Aldrich, Inc., St. Louis, MO, USA) to make a stock solution (10^{-2} M). The stock solution was diluted with ACSF to the appropriate concentration for testing. Rhod-2/AM was purchased from Dojindo Molecular Technologies, Inc. (Kumamoto) and fura-4F/AM was obtained from Invitrogen Molecular Probes (Eugene, OR, USA). According to the product catalogues from Invitrogen, the Ca^{2+} affinities of fura-4F and rhod-2 are 770 and 570 nM, respectively.

Statistical analyses

All data were expressed as means ± S.E.M. Statistical analysis for multigroup data was conducted using Tukey's post-hoc analysis. Paired data obtained from the same slice preparation were analyzed using the paired *t*-test. For comparison between two sets of data obtained in parallel, we employed Student's *t*-test. A *P*-value of less than 0.05 was considered to indicate a statistically significant difference.

Results

Ca^{2+} dynamics during ischemia in cytosol and mitochondria of brain slice preparations detected by fura-4F and rhod-2, respectively

When the slice preparations were exposed to ischemic ACSF (hypoxia and hypoglycemia) by continuous perfusion, the fluorescence signals for the Ca^{2+} level started to

increase within 3 min and gradually increased with time in both $[Ca^{2+}]c$ and $[Ca^{2+}]m$ (Fig. 1: A and B). As shown in the representative recordings (Fig. 1: Aa and Ba), the increase in fluorescence intensity in the LC region occurred earlier than that in the CA1 region. The time courses of the fluorescence signals in the LC and CA1 regions, expressed as the average response obtained from 12 data, are summarized in Fig. 1, Ab and Bb. The average time courses of the fluorescence signal changes in the LC and CA1 regions during ischemia appeared to be

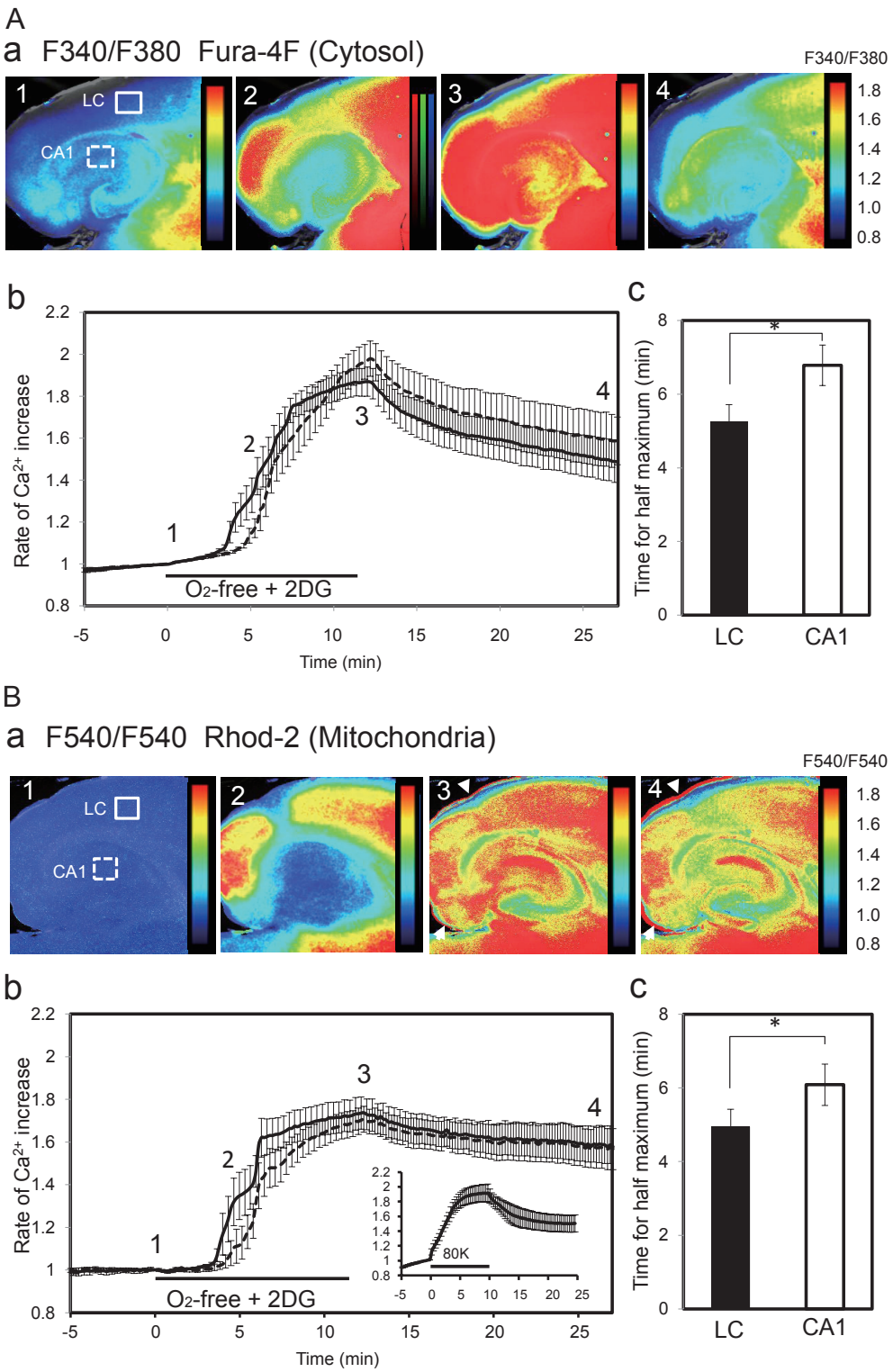

Fig. 1. Time courses of Ca^{2+} concentration changes in mouse brain slice preparations during exposure to ischemic ACSF. Time course of cytosolic and mitochondrial Ca^{2+} concentration changes measured using fura-4F (A) and rhod-2 (B), respectively. a: Representative pseudocolor ratio images (F340/F380 for A, F540/F540 for B) before (1), during (2, 3), and after ischemia (4). Squares on the images refer to ROI. Solid rectangle: lateral cerebral cortex (LC) and broken rectangle: hippocampal CA1 (CA1). b: Average time course of Ca^{2+} concentration changes with S.E.M. bars obtained from 12 experiments. Experimental data were normalized at the level of the start of exposure up to 12 min of ischemia (hypoxia and hypoglycemia), as indicated by a solid horizontal line in each graph. Numbers on each graph refer to those images indicated in panel a. Solid line: LC region and broken line: CA1 region. Inset figure in B: averaged time course of changes in $[Ca^{2+}]m$ with S.E.M. bars (n = 5) as induced by isotonic 80 mM KCl administered for 10 min. Ordinate: rate of Ca^{2+} increase taking the value at the start point as 1.0. Abscissa: time in min. c: Time required for the half maximum increase in the LC and CA1 regions (average ± S.E.M. of 12 data). Filled column: LC region and open column: CA1 region. $*P < 0.05$ using the paired *t*-test. Arrowheads in the images labeled "3" and "4" in Ba indicate the swelling of preparations.

similar. However, the increase in fluorescence intensity in the LC region occurred earlier than that in the CA1 region in every slice preparation tested; thus there was a significant difference in the time for the half-maximum increase in the LC and CA1 regions, when analyzed by the paired *t*-test (Fig. 1: Ac and Bc).

There were no significant differences between the maximum increases in $[Ca^{2+}]c$ and $[Ca^{2+}]m$ in both locations. However, a characteristic difference in $[Ca^{2+}]c$ and $[Ca^{2+}]m$ was observed in the rate of recovery after reperfusion with normal aerobic ACSF. The maximum increase in $[Ca^{2+}]c$ induced within 12 min of ischemia recovered considerably within 15 min of reperfusion. However, the recovery rate of $[Ca^{2+}]m$ from its maximum level after reperfusion with normal ACSF was significantly smaller than that of $[Ca^{2+}]c$ (Fig. 1: Ab and Bb, Table 1). We confirmed that the much higher increase in the rhod-2 fluorescence intensity induced by 80 mM KCl under aerobic conditions could recover by almost 40% within 15 min of washing (see the inset in Fig. 1Bb).

We observed a strong positive fluorescence signal at the edge of the slice preparation during ischemia (arrow heads, No. 3 and 4 images in Fig. 1Ba). The signal might be the result of morphological changes due to swelling in the slice preparation. The signal suggests the development of swelling even after washing (Fig. 1Ba, No. 4).

Effects of CsA and FK506 on ischemia-induced Ca^{2+} dynamics in cytosol and mitochondria

To examine the effects of CsA and FK506 on $[Ca^{2+}]c$ and $[Ca^{2+}]m$ dynamics in mouse brain slice preparations during 12 min of ischemia, we administered the drugs 10 min before, during, and after exposure to ischemic ACSF. The average time course (with S.E.M. bars) in $[Ca^{2+}]c$ and $[Ca^{2+}]m$ of the vehicle control, CsA (10 μM)-treated, and FK506 (10 μM)-treated slice preparations is shown in Fig. 2. Based on the experiments according to the same experimental protocol by changing the drug concentration (0 – 10 μM), we obtained the dose–response relationship to inhibitory effects of CsA and FK506 on the maximum increase in $[Ca^{2+}]c$ and $[Ca^{2+}]m$ in both the LC and CA1 regions (Fig. 3).

CsA significantly inhibited the maximum increase in $[Ca^{2+}]c$ and $[Ca^{2+}]m$ at 10 μM when compared with the vehicle control (Fig. 2: Ab and Bb, Fig. 3: a and c). CsA at 1 μM showed significant inhibitory effects on $[Ca^{2+}]c$ in both the LC and CA1 regions (Fig. 3a) and on $[Ca^{2+}]m$ in the CA1 region (Fig. 3c). A significant inhibitory effect of FK506 could be observed only on $[Ca^{2+}]m$ in both the LC and CA1 regions at 10 μM (Fig. 2: Ac and Bc, Fig. 3d).

CsA and FK506 (10 μM) showed no significant effects on the time for half-maximum increase in $[Ca^{2+}]c$ in the LC and CA1 regions (Fig. 4a). However, both drugs significantly delayed the time for half-maximum increase in $[Ca^{2+}]m$ in the LC region (Fig. 4b). CsA significantly delayed the time for half-maximum increase in $[Ca^{2+}]m$ in the CA1 region, but the effect of FK506 was not significant (Fig. 4b) (Tukey post hoc analysis).

Effects of CsA and FK506 on the abnormal increase in $[Ca^{2+}]c$ and $[Ca^{2+}]m$ induced by high L-glutamate concentration under aerobic conditions

We examined the effects of CsA and FK506 on the abnormal increase in $[Ca^{2+}]c$ and $[Ca^{2+}]m$ induced by high L-glutamate concentration, which would induce severe damage on neuronal cells under aerobic conditions.

We determined the dose of L-glutamate that would induce acute neuronal damage in brain slice preparations. As shown in Fig. 5a, $[Ca^{2+}]c$ increased in a dose-dependent fashion at 5 – 20 mM L-glutamate administered for 5 min, but the responses to 30 mM were apparently weaker than those obtained at 20 mM. The dose–response relationships to L-glutamate observed in $[Ca^{2+}]m$ were complex (Fig. 5b), which showed a U-shape in the range of 5 – 30 mM L-glutamate. We chose 20 mM L-glutamate as the experimental dose to induce acute toxicity in the brain slice preparations.

As shown in Fig. 5c, $[Ca^{2+}]c$ increased during L-gluta-

Table 1. Ca^{2+} dynamics in the cytosol and mitochondria in mouse brain slice preparations following exposure to ischemic ACSF for 12 min

	Cytosol		Mitochondria	
	LC	CA1	LC	CA1
Maximum increase (%)	186.9 ± 7.0	197.1 ± 8.4	173.2 ± 7.4	169.7 ± 6.2
Recovery (%)	47.0 ± 7.8	197.1 ± 8.4	21.3 ± 6.4*	20.3 ± 9.7*

Maximum increase: the percentage response taking the level at the start of ischemia as 100%. Recovery: the percentage of recovery from the maximum increase within 15 min reperfusion. Values are expressed as the average ± S.E.M. using 12 data points. *Statistically significant difference ($P < 0.05$) between the cytosol and the mitochondria in each location (Student's *t*-test).

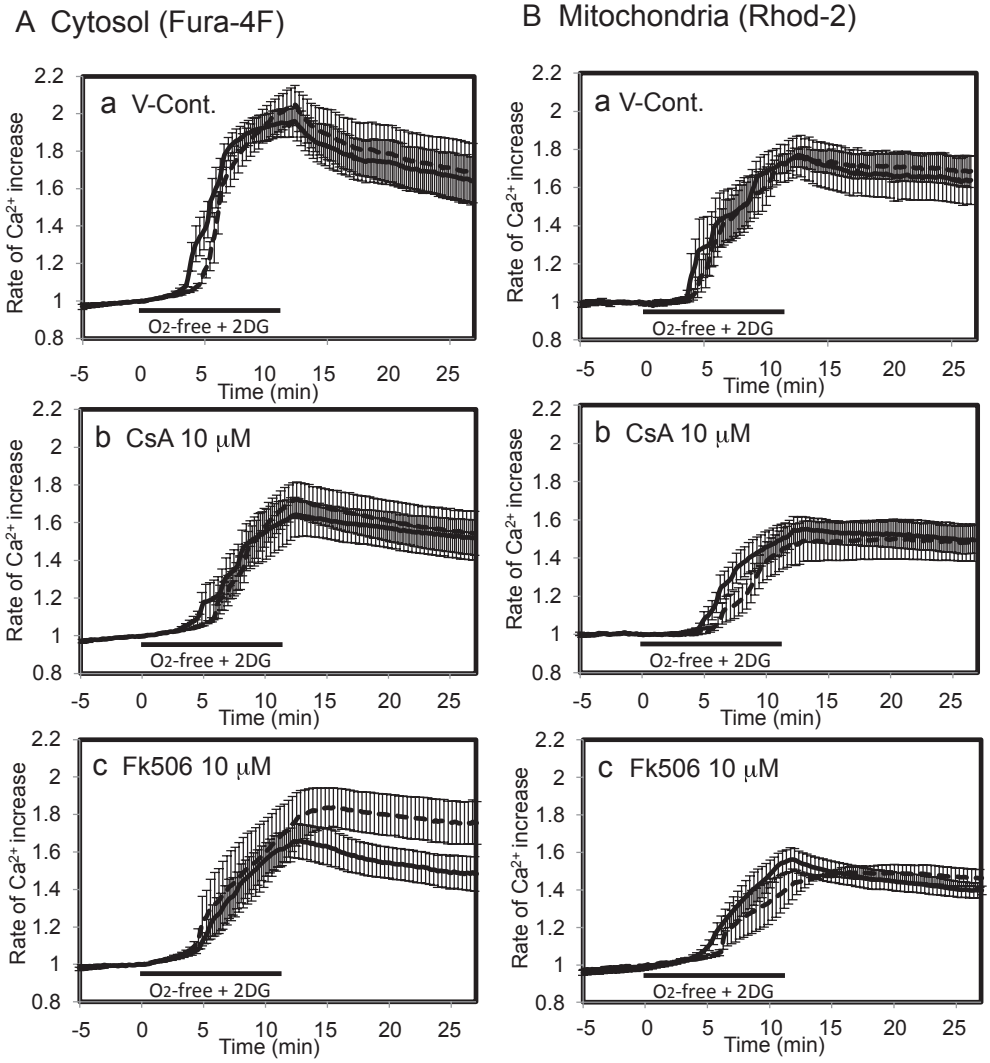

Fig. 2. Effects of CsA and FK506 on the ischemia-induced Ca^{2+} increase in the LC and CA1 regions. Time courses of changes in $[Ca^{2+}]c$ (A) and $[Ca^{2+}]m$ (B) in the slice preparations in vehicle control (0.1% DMSO) (a), treated with 10 μM CsA (b), or FK506 (c) administered 10 min before exposure to ischemic conditions up to the end of the experiment. Each graph represents the average and S.E.M. of 5 (drug-treated) and 7 (vehicle-treated) experiments. Solid line: LC region and broken line: CA1 region. Scales are the same as those in Fig. 1.

mate (20 mM) administration for 5 min. After L-glutamate withdrawal, there were further increases in the LC and CA1 regions. An apparent rebound response was more obvious in the CA1 region than in the LC region. On the other hand, the responses in $[Ca^{2+}]m$ to L-glutamate (20 mM) were more complex. As shown in Fig. 5d, the fluorescence intensity in the CA1 region increased just after exposure to L-glutamate, but it immediately decreased transiently and again increased after washing. The time course of responses to L-glutamate in the LC region was similar to that in the CA1 region, but the fluorescence intensity during L-glutamate exposure in each preparation varied from a small decrease to a pronounced increase.

We examined the effects of CsA and FK506 on the Ca^{2+} dynamics induced by 20 mM L-glutamate, which showed reproducible responses in $[Ca^{2+}]c$. As shown in Fig. 6, CsA and FK506 showed dose-dependent inhibitory effects on responses in $[Ca^{2+}]c$ and $[Ca^{2+}]m$ induced by L-glutamate (20 mM). Statistically significant inhibitory effects on $[Ca^{2+}]c$ in the LC and CA1 regions were observed at 10 μM CsA and FK506 (Fig. 6: a and b). FK506 showed significant inhibitory effects on $[Ca^{2+}]m$ in the LC and CA1 regions at 10 μM (Fig. 6d). The drug also significantly depressed $[Ca^{2+}]m$ in the LC region at 1 μM. CsA was less effective on the $[Ca^{2+}]m$ increase induced by L-glutamate, but showed significant inhibitory effects only on the $[Ca^{2+}]m$ increase in the LC region (Fig. 6c).

Characteristic fluorescence signal changes during administration of high L-glutamate concentration

We examined the fluorescence signal changes in fura-4F induced by 340 nm and 380 nm excitation separately. Although there were evident increases in F340/F380 signals in both the LC and CA1 regions (Fig. 7Aa), the fluorescence signal induced by 340 nm (F340/F340, Fig.

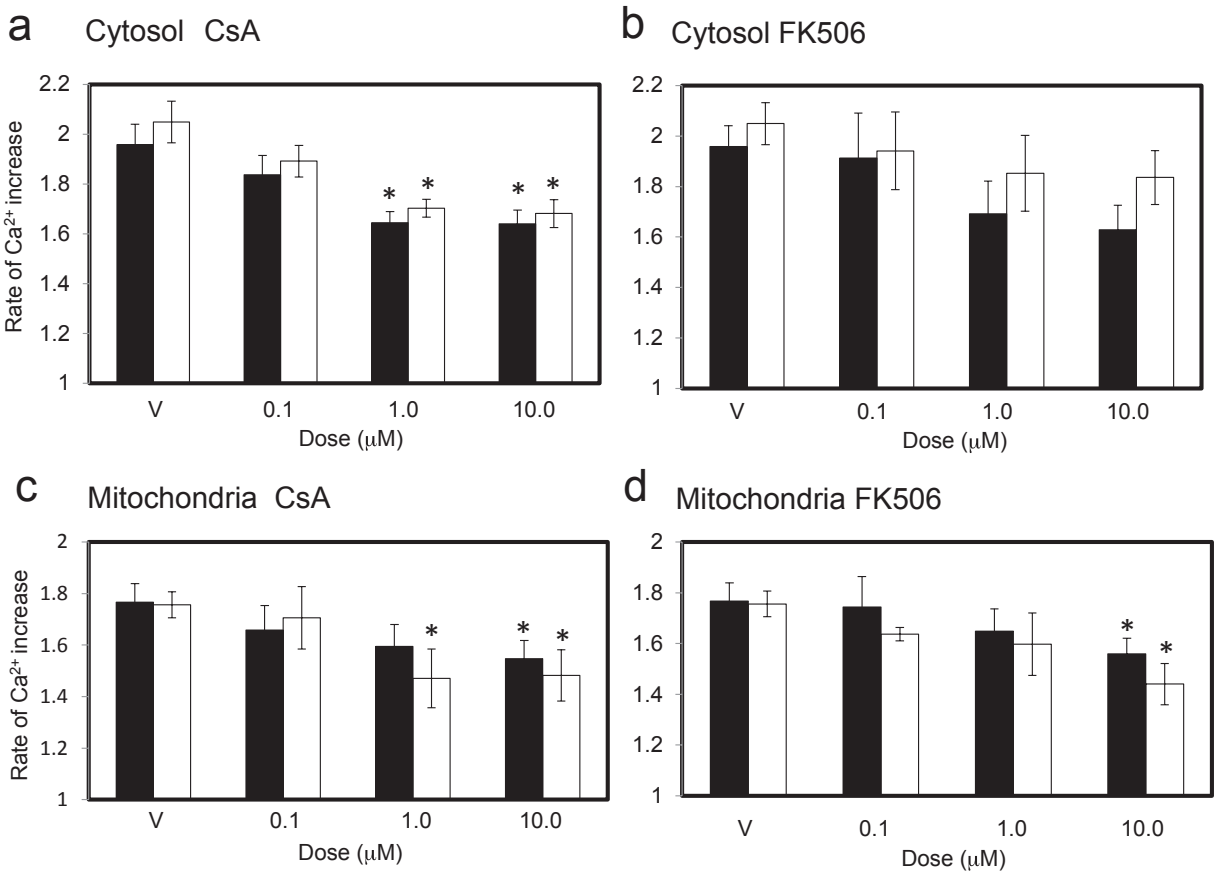

Fig. 3. Dose–response relationships to CsA and FK506 on maximum $[Ca^{2+}]c$ and $[Ca^{2+}]m$ in the LC and CA1 regions. CsA or FK506 (0.1, 1.0, and 10 μM). V: vehicle control, 0.1% DMSO. Values are expressed as the average ± S.E.M. of the maximum increase during ischemia in the slice preparations treated with each dose. Filled columns: LC region and open columns: CA1 region. Each column indicates the average ± S.E.M. values obtained from 5 (drug-treated) and 7 (vehicle-treated) experiments. *$P < 0.05$, by the Tukey post hoc analysis. a and b: Effects of CsA and FK506 on $[Ca^{2+}]c$. c and d: Effects of CsA and FK506 on $[Ca^{2+}]m$. Ordinate: rate of Ca^{2+} increase taking the value at the start point as 1.0.

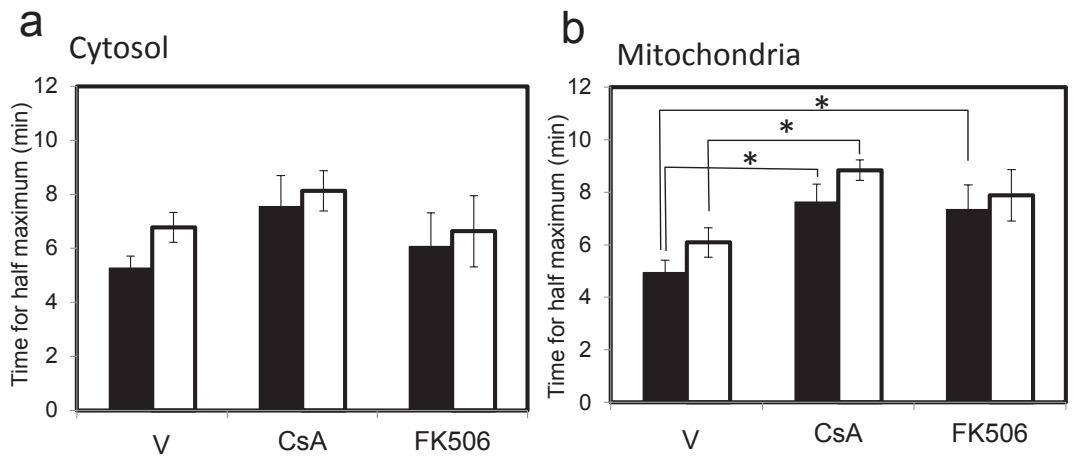

Fig. 4. Effects of CsA and FK506 on the time required for the half maximum increase in the cytosol (a) and mitochondria (b) in the LC and CA1 regions. Filled columns: LC region and open columns: hippocampal CA1 region. Values are expressed as the mean ± S.E.M. of 5 (drug-treated) and 7 (vehicle-treated) experiments. *$P < 0.05$ using the Tukey post hoc analysis compared with the vehicle (0.1% DMSO) experiments.

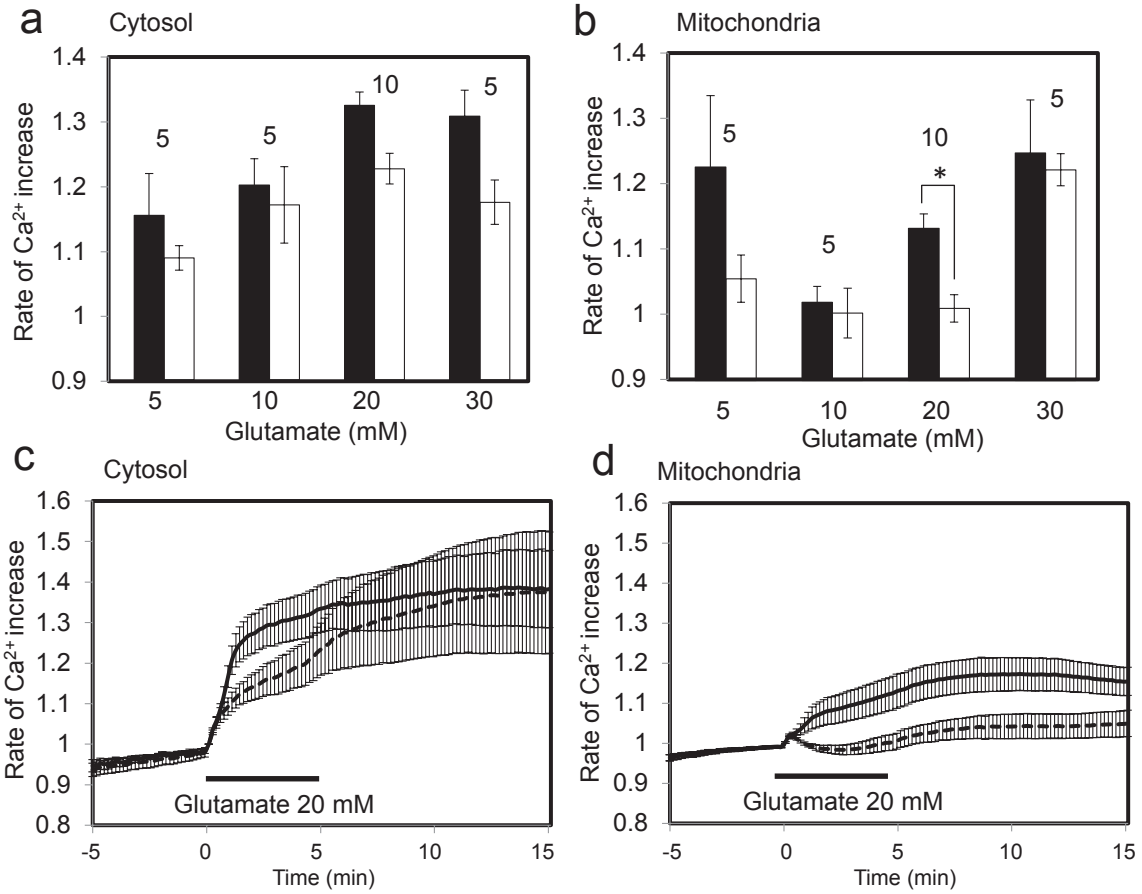

Fig. 5. Effects of high concentrations of L-glutamate on $[Ca^{2+}]c$ and $[Ca^{2+}]m$. Upper panels: Dose–response relationships to L-glutamate from 5 to 30 mM containing 0.1% DMSO on $[Ca^{2+}]c$ (a) and $[Ca^{2+}]m$ (b). Ordinates: the rate of increase of $[Ca^{2+}]c$ and $[Ca^{2+}]m$ at the end of L-glutamate administration. Values are expressed as the average ± S.E.M. Number of experiments performed is indicated on each set of columns. Filled columns: LC region and open columns: CA1 region. $*P < 0.05$, by the paired *t*-test. Lower panels: Time course of average rates of $[Ca^{2+}]c$ and $[Ca^{2+}]m$ (with S.E.M. n = 10) in response to L-glutamate (20 mM) administered for 5 min in fura-4F– or rhod-2–loaded brain slice preparations. Solid line: LC region and broken line: CA1 region. Ordinates are the same as above.

7Ab), which was expected to increase with $[Ca^{2+}]c$ elevation, decreased during L-glutamate (20 mM) administration. The decrease in F380/F380 signals appeared to be greater than the expected signal owing to an increase in $[Ca^{2+}]c$ (Fig. 7Ac).

The fluorescence image (F540) in rhod-2–loaded slice preparations decreased during the administration of L-glutamate (20 mM), but increased after washing. The responses to L-glutamate were always stronger in the CA1 region than in the LC region (Fig. 7B).

We examined the effects of L-glutamate (20 mM) on the slice preparations loaded with MitoTracker Red, which is taken up by mitochondria. Although the fluorescence of the dye should not have any expected substantial responses to environmental changes, it also decreased during L-glutamate administration. The response to L-glutamate was always larger in the CA1 region than in the LC region (Fig. 7C).

A strong signal due to tissue swelling could be observed on the edge of the slice preparations stained by each dye (indicated by arrow heads on W-10 images in Fig. 7: Ab, Ac, B, and C).

Discussion

We set out to examine the protective effects of CsA and FK506 against the abnormal increase in $[Ca^{2+}]c$ and $[Ca^{2+}]m$ in mouse brain slice preparations exposed to ischemic ACSF or high L-glutamate concentration.

Mechanisms of protective effects of CsA and FK506 on abnormal Ca^{2+} dynamics induced by ischemia

We confirmed the protective effects of CsA and FK506 on the abnormal increase in $[Ca^{2+}]m$ induced by ischemia.

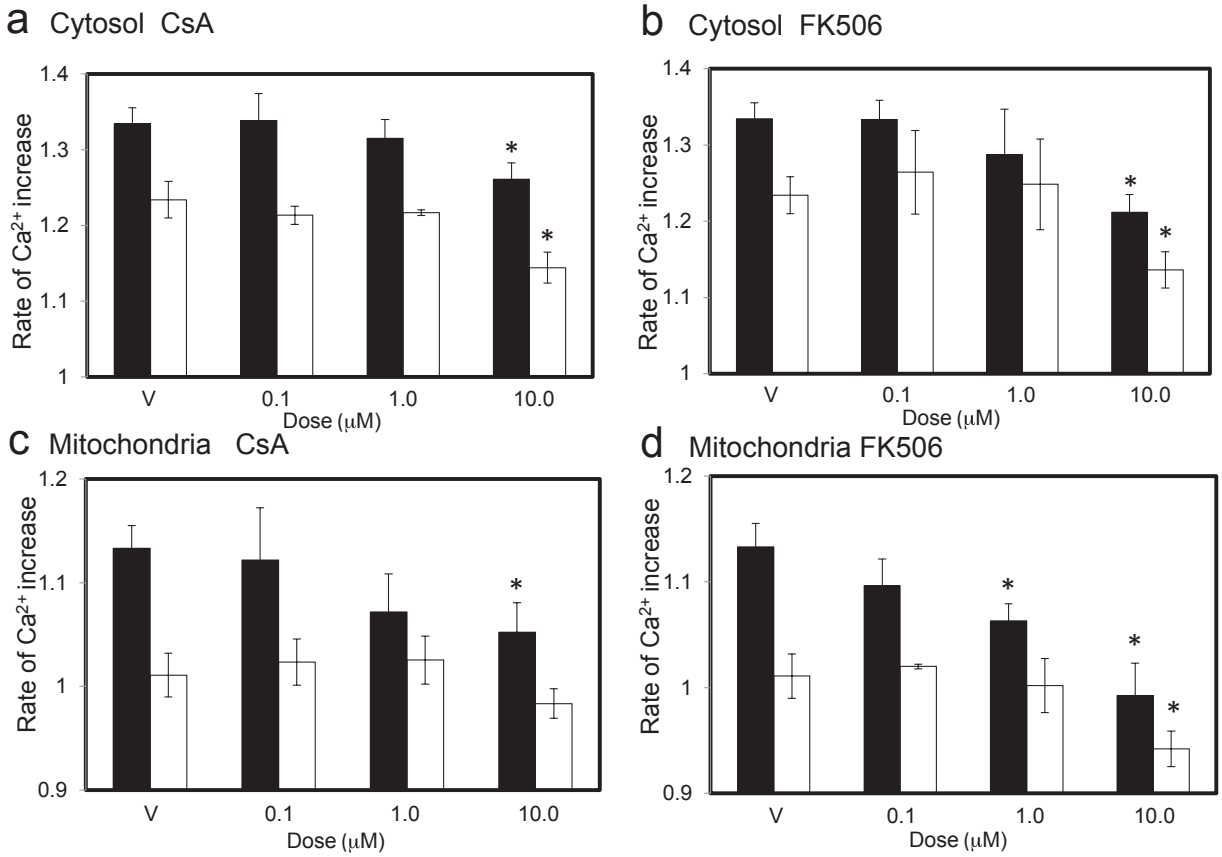

Fig. 6. Dose–response relationships of changes in $[Ca^{2+}]c$ and $[Ca^{2+}]m$ as induced by 20 mM L-glutamate in response to CsA and FK506 treatment. Values for each column are expressed as the average ± S.E.M., n = 5 for each dose of L-glutamate, n = 10 for the vehicle. $*P < 0.05$, by the Tukey post hoc analysis. a and b: Effects of CsA and FK506 on $[Ca^{2+}]c$. c and d: Effects of CsA and FK506 $[Ca^{2+}]m$. Filled columns: LC region and open columns: CA1 region. Ordinates are the same as Fig. 5. Abscissae are doses of CsA or FK506 in μM.

CsA, but not FK506, also significantly protected against the maximum increase in $[Ca^{2+}]c$. These drugs significantly prolonged the time required to reach the half-maximum increase in $[Ca^{2+}]m$, but not in $[Ca^{2+}]c$. These results suggest the preferential effects of both drugs on mitochondrial Ca^{2+} dynamics under ischemic disturbance. CsA was more effective than FK506 in protecting against abnormal Ca^{2+} dynamics.

The protective effects of CsA and FK506 on neuronal damage in experimental brain ischemia have been widely examined, but with conflicting results. Some studies concluded that either CsA or FK506 could protect against ischemic brain damage (23, 35 – 38). However, one study showed that CsA was more effective than FK506 in rescuing neuronal cells from ischemia-induced death (24).

The results of the present study on mouse brain slice preparations demonstrated that the protective effects of CsA and FK506 on Ca^{2+} overloading are substantially the same. The mechanisms of action of these two drugs may be related to their effects as immunosuppressants.

The data obtained by our in vitro study could not be compared directly to the data obtained by in vivo studies, in which the different effects might come from other methodological factors, such as routes of drug administration, methods for inducing focal ischemia, or the timing of evaluation of drug effects.

Reliability of estimation of $[Ca^{2+}]m$ in rhod-2–loaded mouse brain slice preparations

As an indicator for $[Ca^{2+}]m$, we used rhod-2, which is taken up into mitochondria because of its positive charge (39). Although some fraction of rhod-2 may remain in the cytosolic compartment after staining, a large part of the signal from rhod-2 will represent the mitochondrial Ca^{2+} dynamics. To determine the actual $[Ca^{2+}]m$, the data obtained using the rhod-2–loaded preparations should be compared with those obtained from the preparations treated with a protonophore, carbonyl cyanide *p*-(trifluoromethoxy) phenylhydrazone, which causes the

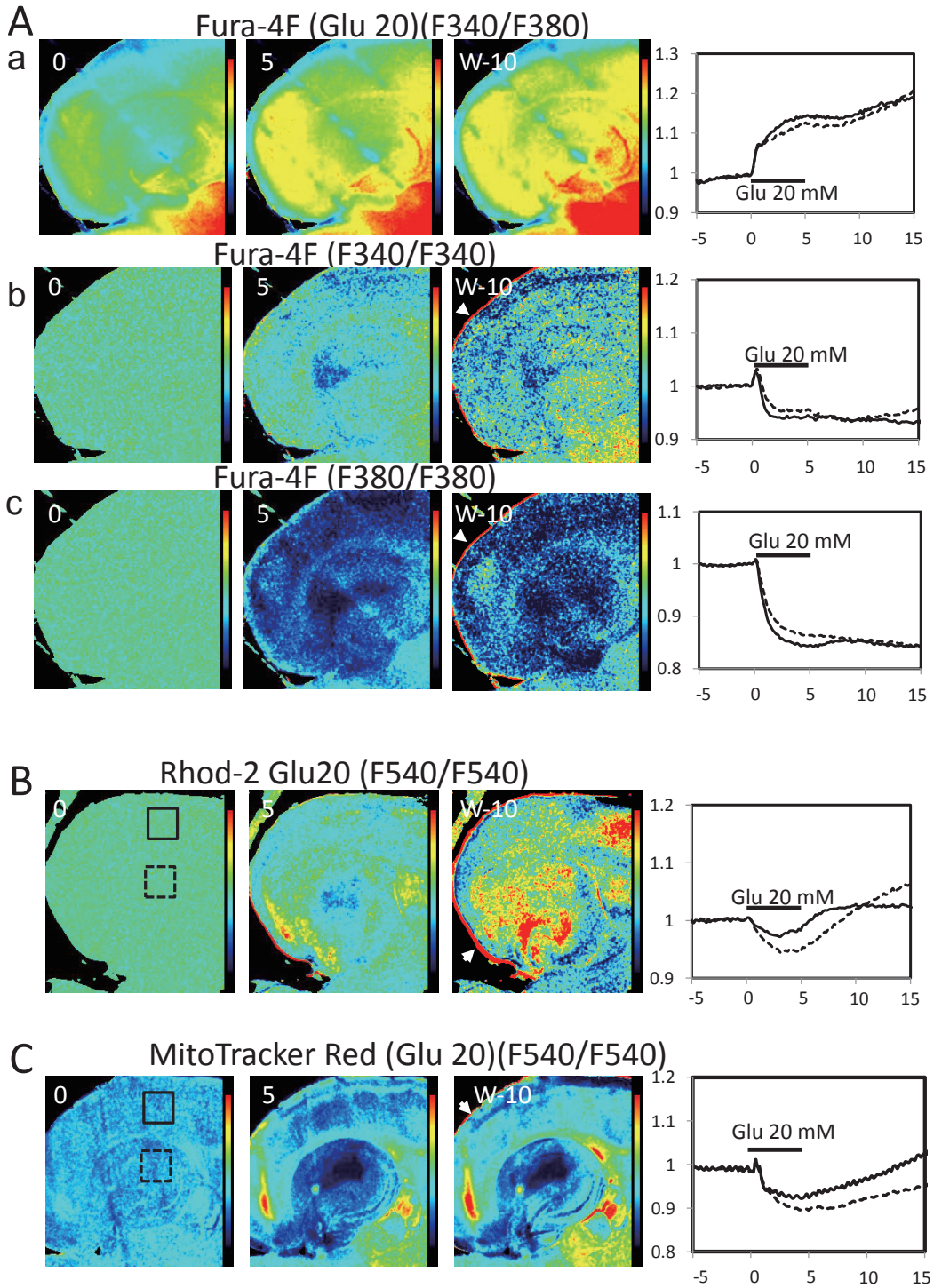

Fig. 7. Fluorescence intensity changes using fura-4F, rhod-2, or MitoTracker Red. A: Ratio imaging of fura-4F–loaded brain slice preparations before ("0" label), after 5 min exposure to L-glutamate (20 mM) ("5" label), and after 10 min of washing-out of L-glutamate (20 mM) ("W-10" label). Fluorescence images (> 500 nm) were obtained by alternative excitation at 340 nm and 380 nm. Three different ratio images were obtained: a) F340/F380, b) F340/F340, and c) F380/F380. B: Ratio imaging of rhod-2–loaded brain slice preparations before ("0" label), after 5 min exposure to L-glutamate (20 mM) ("5" label), and after 10 min of washing-out of L-glutamate (20 mM) ("W-10" label). Fluorescence images (> 580 nm) obtained at 540 nm excitation (F540) were divided by the image obtained at time 0 (F540/F540). C: Ratio imaging of MitoTracker Red–loaded brain slice preparations (F540/F540). Arrowheads in the images labeled "W-10" in Ab, Ac, B, and C indicate the swelling of preparations. The time courses of the changes in fluorescence intensities in the LC and CA1 regions are shown in the right panel. Solid line: LC region and broken line: CA1 region.

mitochondrial membrane potential to collapse (40). Although this method would be effective in cultured cells, it could not be applied to our mouse brain slice preparations because it results in serious damage to the viability of the slice preparations. Instead of using such a drastic method, we estimated $[Ca^{2+}]$m by comparing the results obtained using rhod-2 with the results obtained using fura-4F, a $[Ca^{2+}]$c indicator, in parallel experiments.

The $[Ca^{2+}]$m level observed during ischemia recovered partially (20%) by reperfusion with aerobic ACSF, but the recovery rate was significantly smaller than that of $[Ca^{2+}]$c. This poor recovery rate may be ascribed to the affinity of rhod-2, which might be saturated when there is a maximum increase in $[Ca^{2+}]$m during the ischemic state. We observed that the maximum $[Ca^{2+}]$m induced by 80 mM KCl under aerobic conditions was almost the same or larger than that induced by ischemia, but it recovered by more than 40% after reperfusion with normal ACSF. These results suggest that the poor recovery from maximum $[Ca^{2+}]$m after ischemia might be due to mitochondrial deterioration.

Effects of CsA and FK506 on acute toxicity of L-glutamate

Lang et al. (11) reported that the extracellular glutamate concentration reaches up to 0.2 – 0.5 mM during ischemia, which is 40 – 60 times higher than the resting level (about 5 μM). In the present study, we attempted to examine L-glutamate–induced acute toxicity in mouse brain slice preparations. We found that an extremely high concentration of L-glutamate was required to achieve apparent immediate acute toxicity under aerobic ACSF conditions, in which L-glutamate will be potentially taken up into astrocytes through excitatory amino acid transporters (EAAT) such as GLAST (EAAT1) and GLT1 (EAAT2) (41). We obtained striking responses to L-glutamate in $[Ca^{2+}]$c and $[Ca^{2+}]$m at 20 mM, which appeared excessive compared to the ischemia-induced perturbation. However, we intended to use this concentration as a strategy for elucidating the extreme features of intracellular Ca^{2+} dynamics under aerobic conditions. In this experiment, CsA and FK506 showed almost the same protective effects on both $[Ca^{2+}]$c and $[Ca^{2+}]$m.

The apparent decrease in fluorescence signals in rhod-2 and fura-4F might be dependent on the increased volume of organelles or cells due to the massive water influx in edematous states, and thus the actual concentration of the indicator would be diluted. The results using MitoTracker Red, a marker for living mitochondria, can serve as evidence to demonstrate the transient decrease in fluorescence signals, which is dependent on mitochondrial swelling. A leak of the indicator from the cell or mitochondria would also contribute to the decrease in fluorescence signals. Since the fluorescence signal of fura-4F decreased with only a small recovery, the cellular swelling induced by L-glutamate would persist even after washing out the agent, or some fraction of the loaded indicator might leak out through the edematous cell membrane.

As for mitochondria, mPTPs allow the movement of molecules less than 1500 Da (16). The indicator loaded into mitochondria would leak out through these pore complexes. The fluorescence signals of rhod-2 and MitoTracker Red were reversible by washing with normal ACSF. MitoTracker Red remains inside mitochondria by combining with proteins (42). The similar fluorescence behavior of rhod-2 to MitoTracker Red indicates that part of rhod-2 may remain inside mitochondria even during mPTP opening. These data indicate that the increase in $[Ca^{2+}]$m observed using rhod-2–loaded slice preparations might be distorted by mitochondrial swelling.

Brain edema, which is induced by ischemic or traumatic insult, is an important parameter to evaluate tissue viability. In the present study, we considered the occurrence of edema as swelling in a slice preparation from the false-positive ratio images observed at the edge (note arrowheads in Fig. 1Ba and Fig. 7). The fluorescence intensity tended to increase even after ACSF reperfusion, which had been demonstrated previously by using a specific method (43, 44). CsA and FK506 showed no significant protective effects on the morphological dynamics in cells and mitochondria.

Regional differences in cytosolic and mitochondrial Ca^{2+} homeostasis

Jean-Quartier et al. have reported the cell type specificity of mitochondrial Ca^{2+} uptake (3). On the other hand, we previously demonstrated the difference in the Ca^{2+} capacities of isolated mitochondria between spinal cord and cerebral cortex preparations (45). The present study showed distinct regional differences in Ca^{2+} dynamics between the LC and CA1 regions during ischemia and L-glutamate administration.

Since the preferential vulnerability of the CA1 region to ischemia has already been reported (34), we expected a faster and larger increase in $[Ca^{2+}]$c and $[Ca^{2+}]$m in the CA1 region during exposure to ischemia. Contrary to our prediction, the time course of Ca^{2+} increase during ischemia in the CA1 region was significantly slower than that in the cerebral cortex. Although this is an interesting result, we have no further evidence to explain the meaning of the discrepancy. There were no evident differences in the effects of CsA and FK506 on those areas.

Implications of the present results

Although CsA and FK506 showed significant inhibitory effects on the abnormal Ca^{2+} dynamics induced by ischemia and high L-glutamate concentration, the effects appeared to be rather small. However, the result was not disappointing for us, because the small but significant depressant effects of the drugs on Ca^{2+} overloading under extreme experimental conditions suggested to us that these drugs could still rescue the penumbral region around the damaged area from further deterioration. Furthermore, the depressive effects on the maximum increase and on the time course of increase in $[Ca^{2+}]i$ would delay the process of acute neuronal cell death, and the delay could give us the small, but important chance to rescue the brain from critical damage.

Although our findings based on in vitro Ca^{2+} imaging studies indicated the protective effects of CsA and FK506 on abnormal Ca^{2+} dynamics, further in vivo studies are required to examine whether effective amounts of these drugs are actually delivered into the brain through the blood brain barrier.

Acknowledgments

We are indebted to Dr. Clifford A. Kolba (Ed.D., D.O., M.P.H.), Associate Professor Edward F. Barroga (D.V.M., Ph.D.), and J. Patrick Barron, Chairman of the Department of International Medical Communications of Tokyo Medical University for their editorial review of the English manuscript.

References

1 Berridge MJ, Lipp P, Bootman MD. The versatility and universality of calcium signalling. Nat Rev Mol Cell Biol. 2000; 1:11–21.
2 Graier WF, Frieden M, Malli R. Mitochondria and Ca^{2+} signaling: old guests, new functions. Pflugers Arch. 2007;455: 375–396.
3 Jean-Quartier C, Bondarenko AI, Alam MR, Trenker M, Waldeck-Weiermair M, Malli R, et al. Studying mitochondrial Ca^{2+} uptake - a revisit. Mol Cell Endocrinol. 2012;353:114–127.
4 Perocchi F, Gohil VM, Girgis HS, Bao XR, McCombs JE, Palmer AE, et al. MICU1 encodes a mitochondrial EF hand protein required for Ca^{2+} uptake. Nature. 2010;467:291–296.
5 Hajnóczky G, Robb-Gaspers LD, Seitz MB, Thomas AP. Decoding of cytosolic calcium oscillations in the mitochondria. Cell. 1995;82:415–424.
6 Jouaville LS, Ichas F, Mazat JP. Modulation of cell calcium signals by mitochondria. Mol Cell Biochem. 1998;184:371–376.
7 Duchen MR. Mitochondria and calcium: from cell signalling to cell death. J Physiol. 2000;529:57–68.
8 Yamamoto S, Tanaka E, Shoji Y, Kudo Y, Inokuchi H, Higashi H. Factors that reverse the persistent depolarization produced by deprivation of oxygen and glucose in rat hippocampal CA1 neurons in vitro. J Neurophysiol. 1997;78:903–911.
9 Tanaka E, Yamamoto S, Kudo Y, Mihara S, Higashi H. Mechanisms underlying the rapid depolarization produced by deprivation of oxygen and glucose in rat hippocampal CA1 neurons in vitro. J Neurophysiol. 1997;78:891–902.
10 Uchino S, Nakamura T, Nakamura K, Nakajima-Iijima S, Mishina M, Kohsaka S, et al. Real-time, two-dimensional visualization of ischaemia-induced glutamate release from hippocampal slices. Eur J Neurosci. 2001;13:670–678.
11 Lang D, Kiewert C, Mdzinarishvili A, Schwarzkopf TM, Sumbria R, Hartmann J, et al. Neuroprotective effects of bilobalide are accompanied by a reduction of ischemia-induced glutamate release in vivo. Brain Res. 2011;1425:155–163.
12 Hunter DR, Haworth RA. The Ca^{2+}-induced membrane transition in mitochondria. I. Protective mechanisms. Arch Biochem Biophys. 1979;195:453–459.
13 Crompton M, Barksby E, Johnson N, Capano M. Mitochondrial intermembrane junctional complexes and their involvement in cell death. Biochimie. 2002;84:143–152.
14 Friberg H, Wieloch T. Mitochondrial permeability transition in acute neurodegeneration. Biochimie. 2002;84:240–250.
15 Sullivan PG, Rabchevsky AG, Waldmeier PC, Springer JE. Mitochondrial permeability transition in CNS trauma: cause or effect of neuronal cell death? J Neurosci Res. 2005;79:231–239.
16 Zoratti M, Szabò I. The mitochondrial permeability transition. Biochim Biophys Acta. 1995;1241:139–176.
17 Peres Velazquez JL, Franseva MV, Carlen PL. In vitro ischemia promotes glutamate-medicated free radical generation and intracellular calcium accumulation in hippocampal pyramidal neurons. J Neruosci. 1997;17:9085–9094.
18 Frantseva MV, Carlen PL, Perez Velazquez JL. Dynamics of intracellular calcium and free radical production during ischemia in pyramidal neurons. Free Radic Biol Med. 2001;31:1216–1227.
19 Rordorf G, Uemura Y, Bonventre JV. Characterization of phospholipase A2 (PLA2) activity in gerbil brain: enhanced activities of cytosolic, mitochondrial, and microsomal forms after ischemia and reperfusion. J Neurosci. 1991;11:1829–1836.
20 Yamashima T. Ca^{2+}-dependent proteases in ischemic neuronal death a conserved 'calpain-cathepsin cascade' from nematodes to primates. Cell Calcium. 2004;36:285–293.
21 Lipton P. Ischemic cell death in brain neurons. Physiol Rev. 1999;79:1431–1568.
22 Harada S, Fujita-Hamabe W, Tokuyama S. Ischemic stroke and glucose intolerance: a review of the evidence and exploration of novel therapeutic targets. J Pharmacol Sci. 2012;118:1–13.
23 Uchino H, Elmér E, Uchino K, Lindvall O, Siesjö BK. Cyclosporin A dramatically ameliorates CA1 hippocampal damage following transient forebrain ischaemia in the rat. Acta Physiol Scand. 1995;155:469–471.
24 Uchino H, Minamikawa-Tachino R, Kristián T, Perkins G, Narazaki M, Siesjö BK, et al. Differential neuroprotection by cyclosporin A and FK506 following ischemia corresponds with differing abilities to inhibit calcineurin and the mitochondrial permeability transition. Neurobiol Dis. 2002;10:219–233.
25 Yamaguchi T, Miyata K, Shibasaki F, Isshiki A, Uchino H. Effect of cyclosporin a on immediate early gene in rat global ischemia and its neuroprotection. J Pharmacol Sci. 2006;100:73–81.
26 Gupta YK, Chauhan A. Potential of immunosuppressive agents in cerebral ischaemia. Indian J Med Res. 2011;133:15–26.
27 Liu J, Farmer JD Jr, Lane WS, Friedman J, Weissman I, Schreiber SL. Calcineurin is a common target of cyclophilin-cyclosporin A and FKBP-FK506 complexes. Cell. 1991;66:807–815.

28 Tanveer A, Virji S, Andreeva L, Totty NF, Hsuan JJ, Ward JM, et al. Involvement of cyclophilin D in the activation of a mitochondrial pore by Ca^{2+} and oxidant stress. Eur J Biochem. 1996; 238:166–172.
29 Crompton M, Barksby E, Johnson N, Capano M. Mitochondrial intermembrane junctional complexes and their involvement in cell death. Biochimie. 2002;84:143–152.
30 Sullivan PG, Rabchevsky AG, Waldmeier PC, Springer JE. Mitochondrial permeability transition in CNS trauma: cause or effect of neuronal cell death? J Neurosci Res. 2005;79:231–239.
31 Klettner A, Herdegen T. FK506 and its analogs - therapeutic potential for neurological disorders. Curr Drug Targets CNS Neurol Disord. 2003;2:153–162.
32 Morita K, Kitayama T, Kitayama S, Dohi T. Cyclic ADP-ribose requires FK506-binding protein to regulate intracellular Ca^{2+} dynamics and catecholamine release in acetylcholine-stimulated bovine adrenal chromaffin cells. J Pharmacol Sci. 2006;101: 40–51.
33 Kudo Y, Nakamura T, Ito E. A 'macro' image analysis of fura-2 fluorescence to visualize the distribution of functional glutamate receptor subtypes in hippocampal slices. Neurosci Res. 1991; 12:412–420.
34 Kirino T. Delayed neuronal death. Neuropathology. 2000; 20 Suppl:S95–S97.
35 Shiga Y, Onodera H, Matsuo Y, Kogure K. Cyclosporin A protects against ischemia-reperfusion injury in the brain. Brain Res. 1992;595:145–148.
36 Sharkey J, Butcher SP. Immunophilins mediate the neuroprotective effects of FK506 in focal cerebral ischaemia. Nature. 1994; 371:336–339.
37 Giordani F, Benetolli A, Favero-Filho LA, Lima KC, Cestari Junior L, Milani H. Tacrolimus (FK506) reduces ischemia-induced hippocampal damage in rats: a 7- and 30-day study. Braz J Med Biol Res. 2003;36:495–502.
38 Yoshimoto T, Uchino H, He QP, Li PA, Siesjö BK. Cyclosporin A, but not FK506, prevents the downregulation of phosphorylated Akt after transient focal ischemia in the rat. Brain Res. 2001; 899:148–158.
39 Minta A, Kao JP, Tsien RY. Fluorescent indicators for cytosolic calcium based on rhodamine and fluorescein chromophores. J Biol Chem. 1989;264:8171–8178.
40 Drummond RM, Tuft RA. Release of Ca^{2+} from the sarcoplasmic reticulum increases mitochondrial $[Ca^{2+}]$ in rat pulmonary artery smooth muscle cells. J Physiol. 1999;516:139–147.
41 Sonnewald U, Qu H, Aschner M. Pharmacology and toxicology of astrocyte-neuron glutamate transport and cycling. J Pharmacol Exp Ther. 2002;301:1–6.
42 Poot M, Gibson LL, Singer VL. Detection of apoptosis in live cells by MitoTracker red CMXRos and SYTO dye flow cytometry. Cytometry. 1997;27:358–364.
43 Nakajima R, Nakamura T, Miyakawa H, Kudo Y. Effects of mannitol on ischemia-induced degeneration in rat hippocampus. J Pharmacol Sci. 2004;95:341–348.
44 Nakajima R, Nakamura T, Ogawa M, Miyakawa H, Kudo Y. Novel method for quantification of brain cell swelling in rat hippocampal slices. J Neurosci Res. 2004;76:723–733.
45 Morota S, Hansson MJ, Ishii N, Kudo Y, Elmér E, Uchino H. Spinal cord mitochondria display lower calcium retention capacity compared with brain mitochondria without inherent differences in sensitivity to cyclophilin D inhibition. J Neurochem. 2007;103:2066–2076.